



**CHALMERS**  
UNIVERSITY OF TECHNOLOGY



The S3 stack from PowerCell Group, Photo: PowerCell Group.

# **An investigation into the predictability of membrane durability in Proton-exchange membrane fuel cells**

A research project with PowerCell Group

Master's thesis in Applied Mechanics

**JUSTUS LINDQVIST**

---

DEPARTMENT OF INDUSTRIAL AND MATERIAL SCIENCE  
CHALMERS UNIVERSITY OF TECHNOLOGY  
Gothenburg, Sweden 2023  
[www.chalmers.se](http://www.chalmers.se)



MASTER'S THESIS 2023

**An investigation into the predictability of  
membrane durability in Proton-exchange  
membrane fuel cells**

A research project with PowerCell Group

JUSTUS LINDQVIST



PowerCell Group



**CHALMERS**  
UNIVERSITY OF TECHNOLOGY

Department of Industrial and Material Science  
CHALMERS UNIVERSITY OF TECHNOLOGY  
Gothenburg, Sweden 2023

An investigation into the predictability of membrane durability in  
Proton-exchange membrane fuel cells  
JUSTUS LINDQVIST

© JUSTUS LINDQVIST, 2023.

Supervisor: Gabor Toth, PowerCell Group  
Examiner: Magnus Ekh, Department of Industrial and Material Science

Master's Thesis 2023  
Department of Industrial and Material Science Chalmers University of Technology  
SE-412 96 Gothenburg  
Telephone +46 31 772 1000

Cover: The P-Stack model from PowerCell Group, the state- of art fuel cell stack  
from PowerCell.

Typeset in L<sup>A</sup>T<sub>E</sub>X  
Gothenburg, Sweden 2023

## Abstract

This work addresses the issue of lifetime of the proton exchange membrane, one of the vital components of Proton exchange membrane fuel cells, with a focus on its mechanical and fatigue response under typical operating conditions.

Although the durability of a complete system can only be defined by investigating each of its constituent materials and components, both separately and in combination, the polymer membrane that acts as a gas separator and a solid electrolyte is at the heart of a fuel cell's performance. The mechanical stability of this membrane is the most pressing issue for efficient commercialization of Hydrogen fuel cells, and a large hindrance for achieving longer lifetimes of hydrogen fuel cells is the lack of understanding of its degradation and eventual failure during operation.

To properly evaluate this one needs to a.) determine the in-situ mechanical stresses that develop in the membrane, and b.) to evaluate the effect of the mechanical stress response on the membrane fatigue life. Both of which will be covered in this thesis.

Keywords: PEM; degradation; durability; hydrogen; Membrane; Fuel cell



## Acknowledgements

The author would like to thank Gabor Toth, Felix Ernst, and Caroline Jansson for all their help and guidance at Powercell Sweden AB. I also want to thank Anneli Jedenmalm for performing the DMA testing and Nathalie Davidsson for her help with the text in the report.

Justus Lindqvist, Gothenburg, Februari 2023





# Contents

<b>List of Figures</b>	<b>xi</b>
<b>List of Tables</b>	<b>xiii</b>
<b>1 Introduction</b>	<b>1</b>
1.1 Background . . . . .	1
1.1.1 Applications . . . . .	2
1.1.2 History . . . . .	3
1.2 Problem Statement . . . . .	3
1.3 Significance . . . . .	4
1.4 Scope . . . . .	4
<b>2 Theory</b>	<b>5</b>
2.1 Degradation of PEM . . . . .	5
2.1.1 Hygrothermal aging . . . . .	6
2.1.2 Chemical degradation . . . . .	6
2.1.3 Thermal decomposition . . . . .	7
2.1.4 Contaminants . . . . .	7
2.2 Previous research . . . . .	7
2.2.1 Tensile Test . . . . .	7
2.2.2 Swelling Testing . . . . .	9
2.2.3 The Department of Energy Testing protocol . . . . .	10
2.2.4 Membrane humidity stability factor . . . . .	10
2.2.5 Fatigue life analysis . . . . .	10
2.2.6 Modeling . . . . .	11
2.2.6.1 Modeling the membrane . . . . .	11
2.2.7 Modeling results . . . . .	13
2.2.8 Modeling fatigue . . . . .	16
<b>3 Methods</b>	<b>19</b>
3.1 Selection methodology . . . . .	19
3.1.1 Part 1 . . . . .	19
3.1.2 Part 2 . . . . .	20
3.2 Material measurements . . . . .	20
3.3 Theoretical Model . . . . .	21

3.3.1	Swelling stress . . . . .	21
3.3.2	Fatigue limit . . . . .	22
3.3.3	Mechanical failure index . . . . .	23
3.3.4	Using MFI . . . . .	23
3.4	DMA testing . . . . .	24
3.4.1	Stress measuring phase . . . . .	24
3.4.2	Stress cycling phase . . . . .	25
3.4.2.1	Results and conclusions . . . . .	25
3.4.2.2	Remaining life investigation . . . . .	25
3.4.3	Proposed continuation to DMA stress test . . . . .	26
3.4.4	Procedure description . . . . .	26
3.4.4.1	Sample preparation . . . . .	26
3.4.4.2	Stress measuring phase . . . . .	26
3.4.4.3	Stress cycling phase . . . . .	27
3.5	Comparison with known data . . . . .	27
<b>4</b>	<b>Results and discussion</b>	<b>29</b>
4.1	Part 1. Theoretical model . . . . .	29
4.1.1	Discussion . . . . .	30
4.1.2	Potential Changes . . . . .	31
4.1.3	Fatigue testing . . . . .	31
4.2	Part 2. DMA Testing . . . . .	31
4.2.1	The selection of clean PEM . . . . .	32
4.2.2	Stress Measurement Phase . . . . .	32
4.2.3	Stress Cycling phase . . . . .	33
4.2.4	CCM and PEM comparisons . . . . .	33
4.3	Conclusions . . . . .	34
	<b>Bibliography</b>	<b>35</b>

# List of Figures

1.1	Diagram of a PEMFC[2] . . . . .	2
1.2	Typical stacking method for fuel cells[2] . . . . .	2
2.1	Backscattered electron SEM image obtained from a failed CCM (Carbon coated membrane)[13]. . . . .	6
2.2	Tensile Test setup schematic[19] . . . . .	8
2.3	Example of tensile test result on a PFSA PEM, done according to ASTM D882. . . . .	8
2.4	Rheological depiction of Nafion constitutive model. [23] . . . . .	12
2.5	Geometry used for simulations by Silkberstein [23] . . . . .	13
2.6	Loading history used by Silberstein [23] . . . . .	13
2.7	Hydrated stress, $\sigma_{11}$ on the top and $\sigma_{22}$ on the bottom.[23] . . . . .	14
2.8	Dried stress at t=300, $\sigma_{11}$ on the top and $\sigma_{22}$ on the bottom. [23] . . . . .	15
2.9	Hydrated plastic strains at t=300, $\epsilon_{11}^p$ on the top and $\epsilon_{22}^p$ on the bottom. [23] . . . . .	15
2.10	Dried plastic strains at t=300, $\epsilon_{11}^p$ on the top and $\epsilon_{22}^p$ on the bottom. [23] . . . . .	15
2.11	Stresses induced by different humidity cycles[23] . . . . .	16
2.12	Fatigue factor plotted against maximum relative humidity[23] . . . . .	17
3.1	Strain sweep of a PEM, indicating a start of loss of elasticity at an amplitude of 80 $\mu\text{m}$ (0.8% strain) . . . . .	22
3.2	Visual definition of yield stress[19] . . . . .	23
3.3	Stress results correlated to humidity in DMA [13] . . . . .	25
3.4	Schematic diagram of the dog-bone sample geometry used. . . . .	26
4.1	Normalized ( $\frac{MFI_x}{MFI_A}$ ) results for the 4 reference PEM . . . . .	29
4.2	Results of MFI compared to DOE Testing data of the same PEM . . . . .	30
4.3	Illustration of the different trend lines, MFI is linear and DOE is exponential . . . . .	31
4.4	Stress measurement pre-test results . . . . .	32
4.5	The 3 phases of crack growth, figure from Downing [19] . . . . .	33
4.6	Results from article[13] . . . . .	34



# List of Tables

3.1	Material properties of interest . . . . .	21
3.2	DOE RH Cycling test results of reference PEM to be used for comparison with MFI and DMA results. . . . .	27



# 1

## Introduction

In 1874, in his famous novel *The Mysterious Island*, Jules Verne prophesied the rise of hydrogen in response to the exhaustion of fossil fuels: “I believe that water will one day be used as a fuel, that hydrogen and oxygen, which constitute it, used alone or simultaneously, will provide an inexhaustible source of heat and light of an intensity that coal cannot have [1].” Nearly 150 years later, at a time when the need for change is at its most critical stage, this energy sector is at the center of attention and is enjoying unprecedented acceleration.

### 1.1 Background

Proton exchange membrane fuel cells (PEMFCs) are electrochemical devices capable of capturing the chemical energy released in the reaction between hydrogen and oxygen. In this common exothermic reaction hydrogen and oxygen form water, with the PEMFC capturing the released reaction energy and converting it into electricity with exceptional efficiency [2]. This is accomplished in each single cell by dividing the reactants into two separate reaction chambers, connected by a proton-exchange membrane (PEM) and a circuit for conducting electrons. In a fuel cell, the hydrogen in the anode chamber comes into contact with a catalyst surface that is coated on the PEM, where it splits into proton ions and releases its electrons [3]. The proton ions are then transported across the electrolyte membrane which results in the electrons naturally flowing through the circuit to reunite with them at the cathode side. This flow of electrons is the electricity produced by the PEMFC. A similar reaction takes place on the cathode side of the membrane. Oxygen is catalyzed and after contact with the protons it forms water as the sole exhaust from a PEMFC. These single cells are then commonly stacked to multiply the voltage and improve the efficiency of the system. A visual of this is presented in figure 1.2 below this section. A PEMFC commonly operates at around 80°C and with varying degrees of humidity with higher (>80% Relative humidity (RH)) levels being preferred for durability and performance [4]. A schematic overview of these fundamentals for a single cell is shown below in figure 1.1.

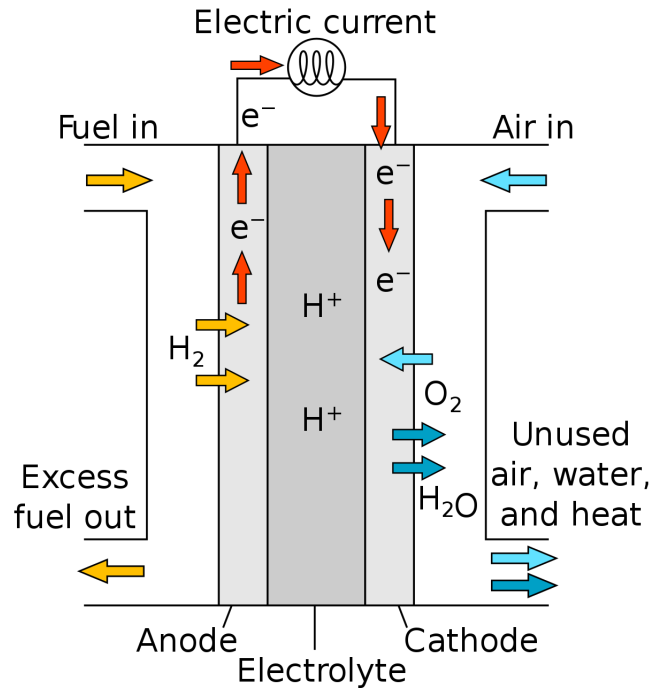


**Figure 1.1:** Diagram of a PEMFC[2]

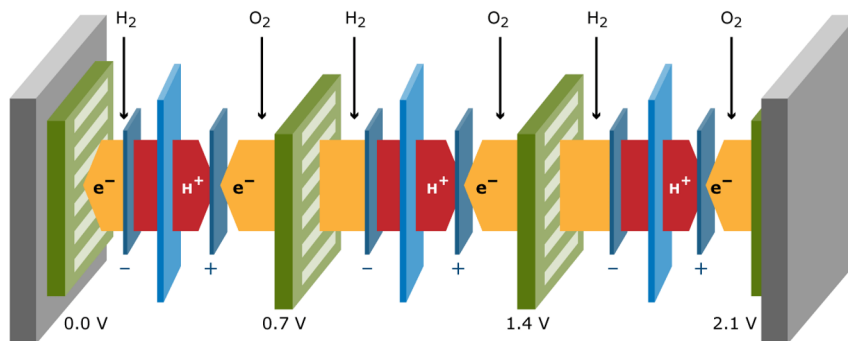


**Figure 1.2:** Typical stacking method for fuel cells[2]

### 1.1.1 Applications

Fuel cell technology is commonly believed to play a major part in the transition away from fossil fuels and combustion engines [5]. Commonly mistaken as a direct competitor to battery technology, it instead more naturally fills the needs of applications where batteries may be ill-suited. Such applications will generally be those where high amounts of energy capacity are required, and batteries become too heavy and/or expensive [6] to be a competitive solution. For such scenarios, PEMFC offers a viable alternative to the Internal combustion engine (ICE) with long range and a high power density [7].



### 1.1.2 History

Fuel cell technology is not a new invention. In fact, General Motors developed the first fuel cell road vehicle, the Chevrolet Electrovan, already in 1966. It had a PEMFC and a range of 120 miles with a top speed of 70 mph. There were only two seats, as the fuel cell stack and large tanks of hydrogen and oxygen took up the entire rear of the van [8]. Nonetheless, the fuel cell industry and PowerCell Group have experienced a rapid increase of interest in their technology [2]. The underlying cause of this increase in attention is two-fold, but both points are rooted in the environmental discussion. Firstly, the IEC that currently dominates the transport sector is becoming less viable, and an alternative is needed as societies are pursuing options with lower emissions [6]. Secondly, with a future energy mix projected to consist of ever more renewable energy sources (RES), hydrogen can provide a scalable storage solution to shift electricity generation in the time domain. An example of this is to utilize wind power to produce hydrogen with the use of electrolyzers when there is an overproduction of electricity. An electrolyser can be described as a fuel cell in reverse, producing hydrogen from electricity and water. This hydrogen can later be used at times of less overproduction to produce electricity again by the use of fuel cells or combustion processes.

## 1.2 Problem Statement

The reason this technology is not yet fully commercialized is due to the pending concerns regarding its lifetime and price-performance ratio [9]. Fuel cells have not yet demonstrated a level of durability comparable to the incumbent technologies in the main application areas of transportation and stationary power generation. In these applications, normal operating conditions can include stress inducing elements such as: impurities in the fuel and air, starting and stopping, freezing and thawing, and humidity and load cycles that result in stress on the chemical and mechanical stability of the fuel cell materials, components and interfaces. While some of the ageing and degradation mechanisms are known, effective mitigation strategies to provide the required lifetime are still lacking [10]. The Department of Energy's (DOE) current target for the lifetime of a PEMFC in an automotive application is 5000 hours [10], a lifetime that is difficult to provide outside of the most favorable operating conditions [2].

It is known that the durability of the PEM is currently the main factor restricting the lifetime of a PEMFC [11]. The complexity of operating conditions described above (such as startup-shutdown, open-circuit/idling and dynamic loading) will cause high amounts of stress and degradation of the PEM, negatively affecting the end service life of the PEMFC [2].

### 1.3 Significance

It is generally accepted that to evaluate the durability of a PEM today, one has to follow something similar to the DOE testing protocols [10] for either mechanical or chemical accelerated stress [2]. The accomplishment of this is both costly and tedious as it requires the assembly of a membrane electrode assembly (MEA), and then potentially thousands of hours of testing [2] if done in accordance with the DOE standard. This issue has previously not received major attention, as there have not been many membrane alternatives to choose from when producing a PEMFC, and the industry has instead focused on improving the system around the PEMFC stack [2]. However, as the industry keeps expanding, more alternatives to the current state of the art PEM are appearing on the market at an exponentially increasing rate [2]. This prompts the commercial need for a higher grade of understanding of the subject, along with a more cost- and time efficient evaluation process.

### 1.4 Scope

The durability of PEM is commonly divided into two categories: mechanical and chemical, (with their respective target values from the DOE). While these always coexist in any real application, they are separated by both the DOE and in the most cited literature [2]. To form a complete understanding of PEM durability is much too large subject for a single thesis, and delimitations have been made to focus the scope and research aim of this work. As such, the less studied and more critical [11] of the two main sources of degradation has been selected - the mechanical stress. The main argument for this decision is that the chemical aspect of the degradation is better understood and it has proven methods to evaluate stability ex-situ. Developing a counterpart of this alongside a good understanding of what parameters affect it is sorely needed for the mechanical durability. The focal points of this research are thus to both add to and summarize the current knowledge of PEM mechanical stability, as well as to create models to better predict later in-situ failure of the membrane. Thus, the end goal of this work is to use these models and create an applicable process for downselection of potential PEM, with a high degree of correspondence to the DOE testing protocol. The proposed methods for realizing this scope are described in chapter 3.

# 2

## Theory

A membrane within a PEMFC device operates at aggressive hygrothermal and chemical conditions (especially at higher potentials) which affect the membrane's integrity [2]. The interactions between the chemical and mechanical failure modes in these devices make it difficult, yet important, to understand the relationship between the different causes of stress and their respective dominant failure modes. There is a multitude of challenges to address pertaining to the durability of PEM. Below will follow a brief summary of the different mechanisms and factors:

- i *Mechanical degradation*, which manifests itself when the membrane is under mechanical stress, either externally applied, or, more commonly, internally generated as the membrane is geometrically constrained while it wants to expand its volume[2].
- ii *Hygrothermal aging*, when a PEM is exposed to elevated humidity and elevated temperature continuous morphological changes can be induced to the membrane.
- iii *Chemical degradation*, commonly in the form of decomposition, often contributed to the free radicals formed during operations.
- iv *Thermal decomposition*, which is the decomposition of the material similar to chemical degradation triggered by elevated temperature.
- v *Contaminants*, i.e. impurities in either the fuel or PEMFC from production.

It is important to understand that these factors and stressors are interrelated, and although they are often functions of the environment as well as of each other, they also impact and enhance one another through their effects. In the following elaboration of these phenomena, a Perfluorosulfonic Acid (PFSA) membrane will be used as an example, as it is currently regarded as the industry standard PEM [3].

### 2.1 Degradation of PEM

Through the analysis of the failed membranes, with regards to their failure modes and location, the most common mechanical degradation mechanisms of PEM have been defined. These include material fatigue, creep and the generation of wrinkles, delamination, pinholes or cracks. A post-mortem analysis using a sweeping electron microscope (SEM) is showcased below in figure 2.1. These mechanical degradation mechanisms of the membrane are generally considered to be the main reasons for the early failure of fuel cells [12]. For example when a pinhole is formed the reac-

tant gas crossover becomes uncontrollable. While there are many reasons for the mechanical failure of PEM (such as improper structural design, uneven assembly and unsuitable material matching), the main source of the stress, both uniform and locally concentrated, is the repeated swelling and contractions induced through the cycling of humidity and temperature that occurs during operations.

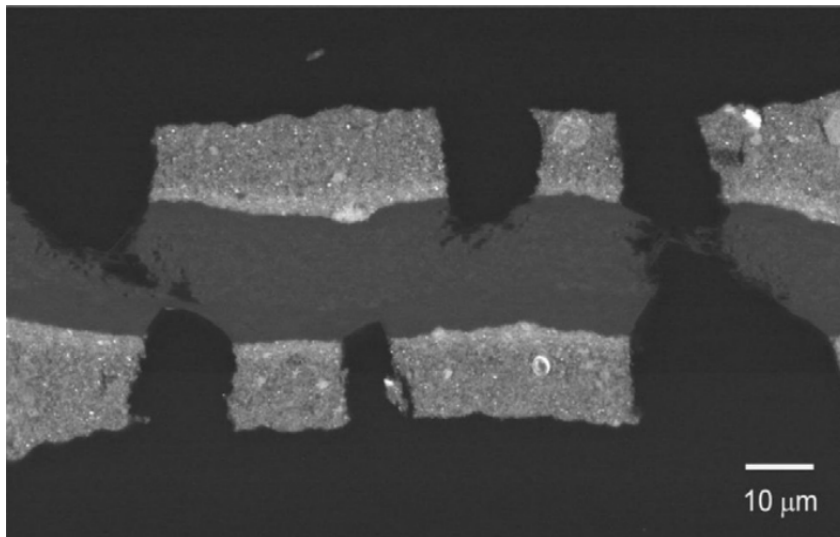


**Figure 2.1:** Backscattered electron SEM image obtained from a failed CCM (Carbon coated membrane)[13].

### 2.1.1 Hygrothermal aging

A PFSA membrane is not at a true chemical equilibrium [2], therefore their morphology tends to change over time and under certain environmental conditions. If the changes happen over a long time, they are then called aging. The effects are enhanced during higher levels of humidity (operations) and give a theoretical maximum lifetime of a current PEM. However, for the current state of the art PEMFC, this is not a large contributing factor to overall degradation, and thus, this is not currently the focus of development [2].

### 2.1.2 Chemical degradation

Proton exchange membranes can chemically decompose via chain-scission and/or chain-unzipping due to attacks by free radical species generated during cell operation. Such degradation has been confirmed in spectroscopic studies[3] and the main culprit is hydroxide radical ( $\cdot\text{OH}$ ) stemming from decomposition of formed hydrogen peroxide (mainly due to hydrogen gas crossover).

The subject of chemical degradation is more well-studied than the other main mechanism for premature failure (mechanical stress), and both the scientific understanding of the stressors and how to measure PEM resistance towards premature failure is thoroughly documented [14, 15].

### 2.1.3 Thermal decomposition

The thermal decomposition of PEM is one of the main reasons for the low operating temperatures of the current industry standard PEMFC [16]. This effect is usually contributed to the low glass-transition temperature of PFSA membranes. Like most other materials, with higher levels of temperature, the glass-transition causes a PFSA membrane to become increasingly soft and lose its stiffness. This in turn amplifies the damage caused by other degradation mechanisms exponentially [2].

### 2.1.4 Contaminants

Contamination of trace amounts of foreign cations can critically affect a PFSA's transport properties and thermomechanical stability. The cations commonly arise from either cell corrosion (e.g. bipolar-plate corrosion), or from balance-of-system components (e.g. seal or tubing degradation). While these are important issues, they ultimately fall outside the scope of this study, as they are much more closely related to the chemical degradation of PEM.

## 2.2 Previous research

As stated, the current research progress made on the mechanical strength of PEM is overall lackluster, and has historically received less focus than the chemical counterpart [11]. It is also common within research and development of PEM, that the discussion is not centered around the durability at all [2]. On the contrary, the focus is often shifted towards the performance and possible efficiency, neglecting the potentially more important topic of lifetime [3]. It is known that relative humidity (RH) cycling exacerbates the mechanical degeneration, and that the in-plane swelling is a main focal point for improving the lifetime for such testing. However a more complete understanding of the failure process is yet to be developed.

The data presented for novel research of PEM mechanical strength is often the results from a Tensile test. This testing procedure measures some basic mechanical variables of the material, but it often lacks insight in why the test has been made, and how any of the variables can be correlated to the later in-situ behaviour of the PEM. Another fault of such testing, not often mentioned, is that these tests are commonly conducted in ambient conditions (23 °C & 50% RH), when the later in-situ conditions are as mentioned closer to 80 °C & 80% RH. A PFSA PEM is a visco-elastic material, and as such, its material properties are heavily affected by the surrounding temperature and humidity [17]. Nevertheless, the tensile test will now be explained, as it is the most common mechanical test presented within PEM research and development [13].

### 2.2.1 Tensile Test

A tensile test is performed by measuring the stress response of a material corresponding to an applied strain, allowing for a variety of properties to be measured

and/or calculated [18]. A typical testing setup is showcased below in figure 2.2

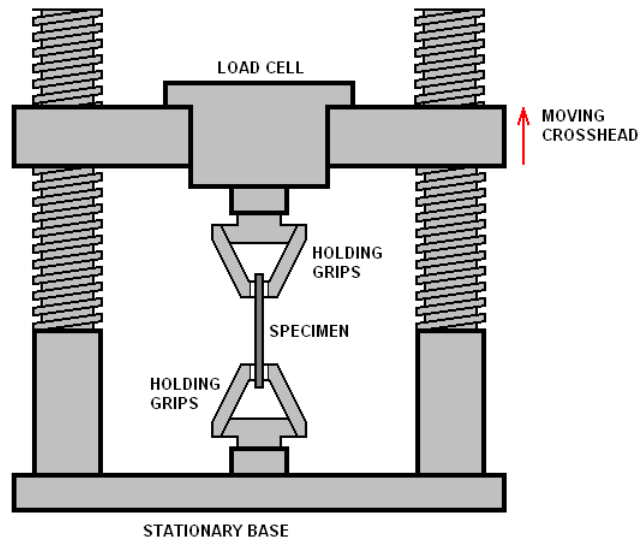


**Figure 2.2:** Tensile Test setup schematic[19]

The test is conducted by pulling the grips apart by a constant rate of separation, measuring the force which is converted into stress by division of the sample cross-sectional area. The strain is measured by use of a Strain gauge. Such a device works on the principle of electrical conductance and its dependence on the conductor's geometry. A strain gauge is a conductor that allows for deformation, allowing the strain to be accurately measured by this change in conductance.

A results plot for a reference PFSA PEM is shown in figure 2.3. A test like this should always follow a procedure standard, for thin materials like these, ASTM D882 (American Society for Testing and Materials) is commonly used [20].

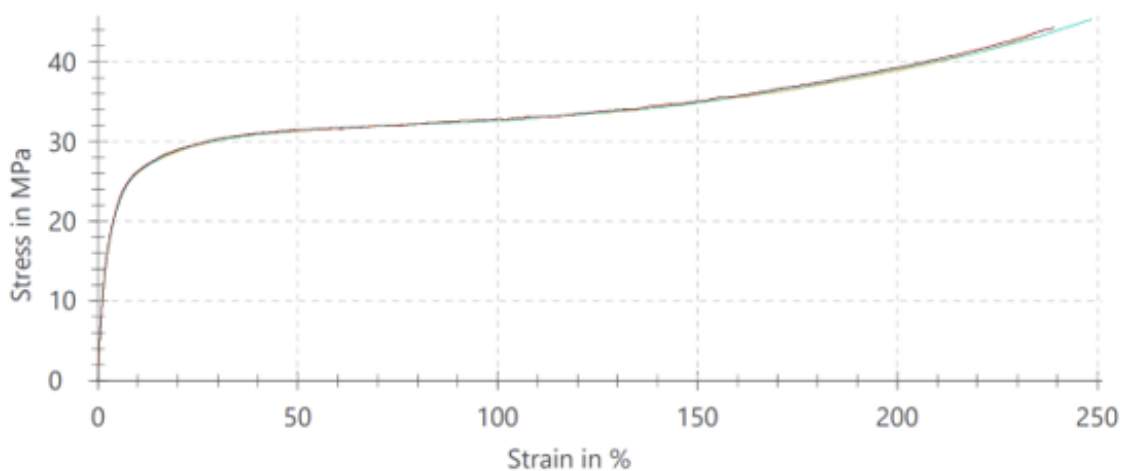


**Figure 2.3:** Example of tensile test result on a PFSA PEM, done according to ASTM D882.

In accordance with standard ASTM D882, the test adopts the engineering stress

and strain for plotting and evaluation of variables. These are calculated as: 2.1-2.2.

$$\sigma = \frac{F}{A_0} \quad \text{Engineering Stress} \quad (2.1)$$

$$\epsilon = \frac{\Delta L}{L_0} \quad \text{Engineering Strain} \quad (2.2)$$

Here  $A_0$  is the original undeformed cross-sectional area,  $L_0$  the undeformed length and  $\Delta L$  the change in length. The material properties most commonly measured by the test are

<i>Property</i>	<i>Definition</i>	<i>Example value from test in figure 2.3</i>
Tensile Strength	The highest measured stress, the stress required to induce failure.	$\approx 45$ MPa
Strain to failure	The highest measured strain, the elongation required to induce failure.	$\approx 245\%$
Yield Stress	The stress required to initiate deformation not reversible by removal of load.	10-15 MPa Depending on definition
Yield Strain	The strain required to initiate deformation not reversible by removal of load.	1-3 % Depending on definition
Young's Modulus	The stiffness of the material for small deformations, calculated as the stress-strain slope for the early regions of deformations.	$\approx 500$ MPa

While this type of test is valuable and more standardized material data is overall needed, a larger understanding of why these variables matter along with models for explaining how they impact a PEM lifetime is needed. A test like this provides no insight into later in-situ behaviour since the, among other things, proper fatigue tests would also be needed to conduct.

### 2.2.2 Swelling Testing

It is well understood that the mechanical strength of PEM is challenged by the stress stemming from the swelling, induced by the high levels of humidity and the following water uptake [2]. This swelling is inhibited by the geometrical constraints, internally generating a stress response by/on the PEM. When following the DOE testing protocol for mechanical stability, this is what is directly cycled until failure is detected through a drastic increase in gas crossover [10].

To measure the magnitude of this property, no ASTM standard exists, but there is an often applied chain of thought in the industry. The dimensions of the PEM is first measured in ambient condition, the membrane is then submersed in water of  $\approx 80^\circ\text{C}$  (to replicate typical in-situ conditions) for a period of time. After this the dimensions are measured again and any apparent changes are labeled as PEM swelling.

### 2.2.3 The Department of Energy Testing protocol

The DOE Testing protocol is the most developed procedure for evaluating the in-situ lifetime of a membrane electrode assembly (MEA, a catalyst coated PEM). The procedure uses a single cell (or stack) and cycles the humidity between 0 and 90% RH while holding a temperature of 80°C [10]. This testing procedure, while accurately measuring the PEM’s mechanical stability, is both expensive and tedious, often taking upwards of 100 days. Along with the rapidly expanding market of suppliers, this prompts the need for a more predictive model in combination with an improved understanding of the degradation phenomena. A procedure that could be used to evaluate the membranes at an earlier state of product development would be helpful in accelerating the progress of PEMFC.

### 2.2.4 Membrane humidity stability factor

Established by MacKinnon et al[21], on behalf of General Motors in 2009, the humidity stability factor ( $F_x$ ) is one of the few attempts at creating a theoretical model based on ex-situ testing data to predict the later in-situ mechanical stability of PEM [21]:

$$F_x = \frac{\%Strain\ to\ failure}{\%Swelling} \quad (2.3)$$

With Strain to failure measured in ambient conditions according to ASTM D882, and Swelling measured as explained in section 2.2.2. It is described by MacKinnon “as a metric of the likelihood of a membrane to withstand repeated humidity cycling.”[21] The variable has no intrinsic value and/or unit and can only be used to numerically compare two PEM as more or less likely to fail mechanically. Such an approach is interesting and this report aims to improve upon this perspective. If the swelling is = 0, the risk of swelling induced failure would also be = 0, and so then the resistance is =  $\infty$

### 2.2.5 Fatigue life analysis

Understanding the lack of validated ex situ methodology to characterize membrane durability under humidity cycling (mechanical stability), T.T. Aindow and J. O’Neill proposed in 2010 that that the stress applied in Dynamic mechanical analysis (DMA) tests could be translated to the one experienced by PEM during fuel cell operation [13]. In DMA testing, a small deformation is applied to a sample in a cyclic manner. This allows the material’s response to stress, temperature, frequency and other values to be studied. The device is otherwise mainly used in combination with a temperature sweep to measure a material’s loss of elasticity as a function of temperature. T.T. Aindow presented the following novel test: Using a DMA equipped with both a humidity and temperature control function, their idea was that it could potentially both measure the stress of swelling, and then cycle it until failure. This original idea will serve as an inspiration for the method applied in this study, and will be further discussed in section 3. Another article was presented in 2014 in cooperation with Ballard power systems where a similar methodology was implemented



with the DMA, which again showcase the validity of such an approach.

## 2.2.6 Modeling

Modeling studies of the in-situ behaviour of PEM are not common. Some attempts have been made and only few attempts have come far enough to implement failure modes of novel materials [2],[22]. Nevertheless they can serve to improve the understanding by providing visual representation of the stress inducing phenomena. A commonly cited work was produced at Massachusetts Institute of Technology by Boyce and Silberstein [23]. In their work, the stress condition was modelled of a PEM made of Nafion. This material stems from the late 60's and it is well studied and it has been considered state of the art for PEM for a long time, though nowadays much competition for that spot exists. The model used the finite element method (FEM) and it was applied to simulate the stress condition of a PEM within the constrained loading conditions of a fuel cell. The geometry used in these simulations are shown below in figure 2.5. The 25  $\mu\text{m}$  thick membrane is perfectly bonded to a 100  $\mu\text{m}$  thick Gas diffusion layer (GDL) to form the sandwiched membrane electrode assembly (MEA). This MEA is placed between aligned bipolar plates and the land and the vertically open channel are both 0.5 mm long. The repeating nature of the unit cell is captured with symmetry boundary conditions where the MEA is not allowed to expand or contract in the horizontal direction. A constant force in the vertical direction of 1 N per unit mm depth corresponding to a nominal stress of 1 MPa per total area was added to simulate a typical stack compression. The results were found to be qualitatively insensitive to the force applied to the bipolar plate. Plane strain was assumed in the third dimension, creating a bi-axial loading condition in the membrane plane. The bipolar plate was taken to be rigid and the GDL are modeled as isotropic linear elastic. The membrane was subjected to a uniform history of water content and temperature changes as showcased in figure 2.6 where is the water content is varied from  $1.5\lambda$  to  $22\lambda$  (Moles of water per mole of sulfonic acid group, typically used measurement for PEM hydration) and the temperature is varied from  $25^\circ\text{C}$  to  $85^\circ\text{C}$  [23]. These conditions accurately reflect both the in-situ situation of operations and the DOE in-situ humidity cycling stability test. [10]

### 2.2.6.1 Modeling the membrane

The swelling of a bimaterial Nafion/GDL strip was selected to derive the constrained swelling and hydration dependant mechanical stress conditions and to evaluate the models ability to capture this behaviour. The membrane will attempt to swell in all directions, but the GDL will constrain expansion in-plane, resulting in a net compressive force in the membrane and a tensile balancing force on the GDL. These equilibrium conditions will cause the composite bilayer strip to bend. This bimaterial test has recently been used to estimate stress levels experienced by the membrane due to constrained swelling [23]. The Stoney formula provides an expression for the curvature ( $\kappa$ ) of a bilayer of a substrate with a stressed thin film:

$$\kappa = \frac{6f}{E_s h_s^2} \quad (2.4)$$

where  $f$  is the film force per unit membrane width,  $E_s$  is the substrate modulus and  $h_s$  is the respective thickness. The film force is a result of the strain mismatch from the swelling. The stress may arise from elastic or inelastic behavior of the membrane where the force is the product of the average membrane stress and the membrane thickness. For the case of a elastic perfectly plastic membrane with yield stress  $\sigma_{y,f}$ ,  $f = \sigma_{y,f}h_f$  Eq: 2.4 then provides a simple relationship to either obtain the curvature given the material behavior, or to obtain the membrane force given the curvature.

$$\kappa = \frac{6\sigma_{y,f}}{h_s E_s} m \eta (1 + \eta) \quad (2.5)$$

where  $\kappa$  is the curvature,  $m = E_f/E_s$  is the elastic modulus ratio,  $\eta = h_f/h_s$  is the thickness ratio. The three-dimensional constitutive model of Nafion, used by Silberstein and Boyce in this article and developed in their previous works, will only be shortly explained here. It was developed and implemented as a user material subroutine in the finite element program Abaqus, monotonic and cyclic uniaxial tension experiments over a range of strain rates and environmental conditions were used to fit and validate the model. The elastic-viscoplastic constitutive model is depicted rheologically in figure 2.4. It includes an intermolecular deformation mechanism (Mechanism I) acting in parallel with a molecular network alignment mechanism (Mechanism N). The intermolecular mechanism, rheologically depicted as an elastic spring in series with a viscoplastic dashpot (P), is the resistance to deformation due to the intermolecular interactions, where the spring captures the stiffness and the dashpot the yielding of these interactions. The intermolecular mechanism has a back stress (B) on the viscoplastic element which develops during loading to assist inelastic recovery.

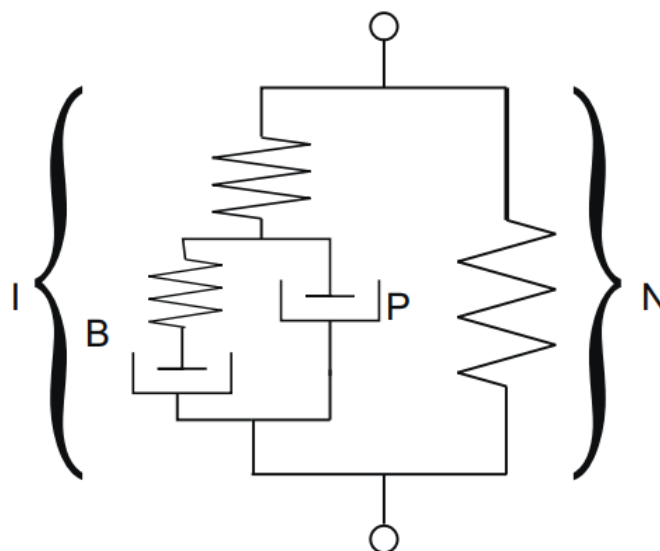


**Figure 2.4:** Rheological depiction of Nafion constitutive model. [23]

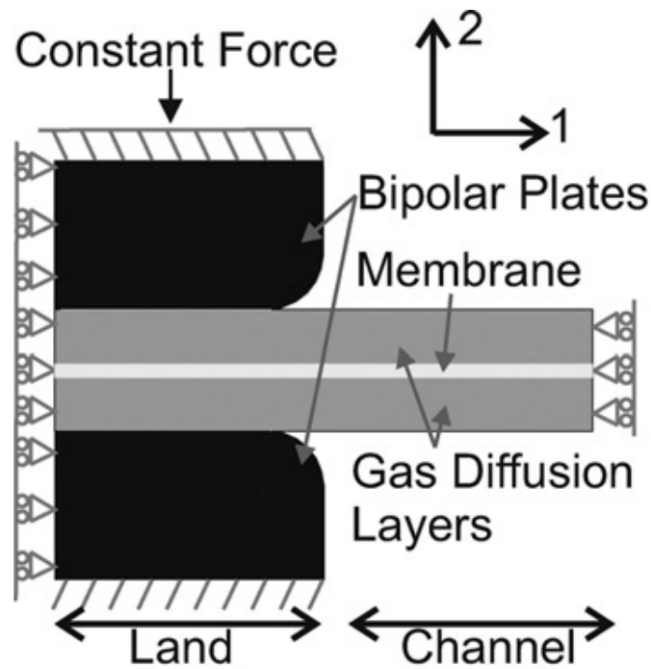


**Figure 2.5:** Geometry used for simulations by Silkberstein [23]

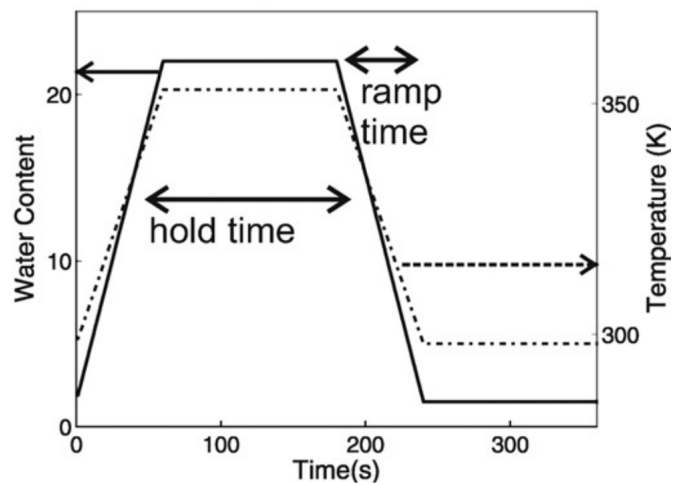


**Figure 2.6:** Loading history used by Silberstein [23]

In figure 2.6 the hydration (solid line) and temperature (dashed line) applied to the model is showcased. The exact time at which the following results are taken is not specified in the article.

### 2.2.7 Modeling results

When the membrane is hydrated within the fuel cell, the constrains of the GDL and the bipolar plate inhibit the swelling, resulting in significant stress ( $\sigma$ ) in the membrane. Representative  $\sigma_{11}$  and  $\sigma_{22}$  contours for the hydrated state are shown below in figure 2.7, top and bottom respectively.

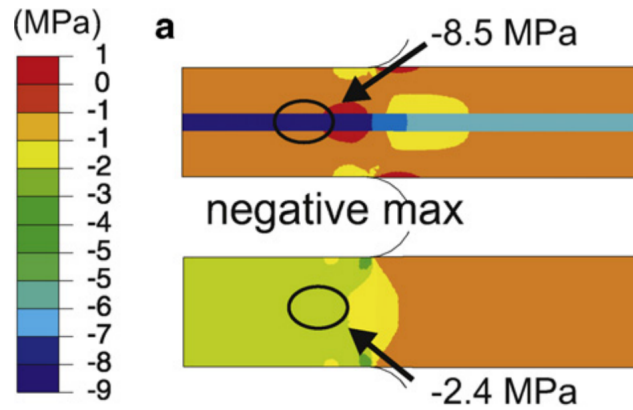


**Figure 2.7:** Hydrated stress,  $\sigma_{11}$  on the top and  $\sigma_{22}$  on the bottom.[23]

During the hydrated step ( $t = 100$ ) The membrane experiences compressive stress in both the 1- and 2-directions are showcased in figure 2.7.  $\sigma_{22}$  is largest beneath the land where the membrane is directly compressed by the clamping force essentially giving a compressive stress of 2 MPa, because neither the membrane or GDL swells significantly in the out-of plane direction, the 2- direction stress is similar in both layers. The hydrated stress in the 1- direction in these simulations on the other hand is much larger in the membrane comparatively. This is because membrane swells significantly in-plane. The results of the later dried state for  $\sigma_{11}$  and  $\sigma_{22}$  are shown in figure 2.8.  $\sigma_{22}$  is compressive and again largely dependent on the applied force constraints.  $\sigma_{11}$  is tensile throughout the membrane and largest just inside the channel. This tensile stress arises due to prior plastic deformation of the membrane during the hydration process. The plastic strain ( $\epsilon^p$ ) in the hydrated and dried states is shown in figures 2.9-2.10. In both states  $\epsilon_{11}^p$  is negative throughout the membrane and  $\epsilon_{22}^p$  is positive. Both of these components of the plastic strain are greater in the channel as a result of the reduced constrain/pressure and larger Mises stress. This effect is more exaggerated for a larger constant force constrain. The development of the plastic strain and the resulting tensile stress during cycling strongly supports the concept of mechanical fatigue driven PEM failure in fuel cells. One of the more subtle aspects of this in-situ modeling is that while the hydration process causes swelling strains, the elastic and plastic strength of the membrane are being reduced as a result of the increase of the water content and temperature. Consequently, similar magnitude stress levels in the hydrated and dried states are likely to cause more plastic deformation in the hydrated state.

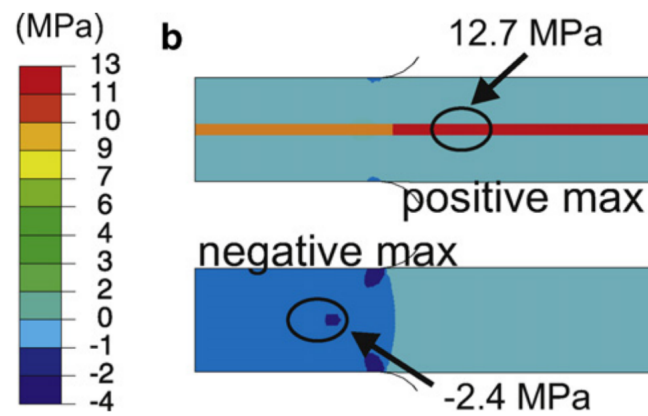


**Figure 2.8:** Dried stress at  $t=300$ ,  $\sigma_{11}$  on the top and  $\sigma_{22}$  on the bottom. [23]

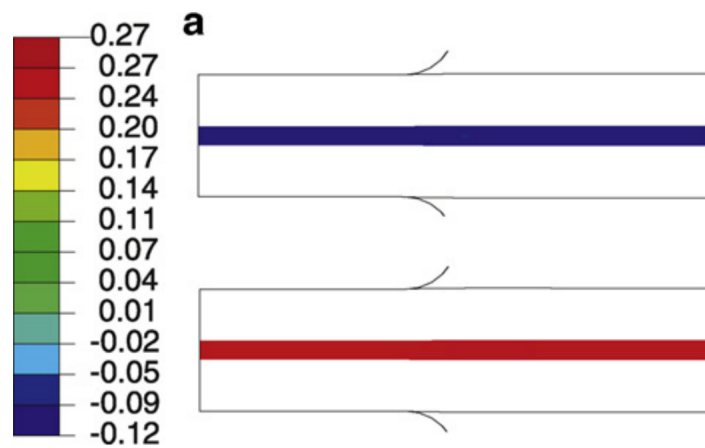


**Figure 2.9:** Hydrated plastic strains at  $t=300$ ,  $\epsilon_{11}^p$  on the top and  $\epsilon_{22}^p$  on the bottom. [23]

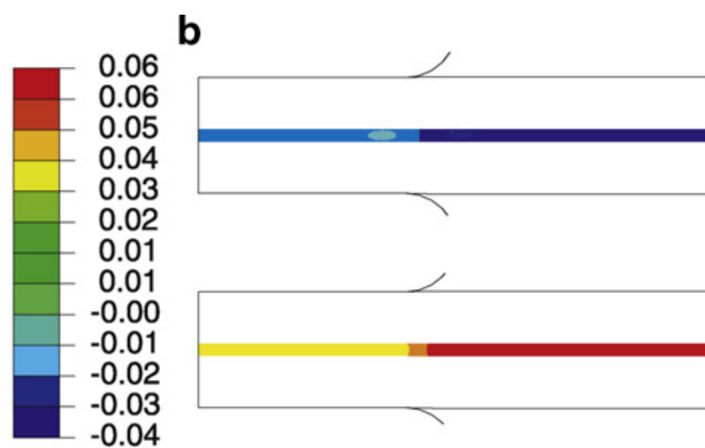


**Figure 2.10:** Dried plastic strains at  $t=300$ ,  $\epsilon_{11}^p$  on the top and  $\epsilon_{22}^p$  on the bottom. [23]

Although neither failure nor fatigue is modeled here it is useful to compare this bi-axial stress, which is on the order of 10 MPa in the dried state, with the material properties of the PEM used. Nafion as used in this study has been shown to have a yield strength of around 8-10 MPa, meaning this stress is high enough to potentially warrant a low-cycle fatigue analysis as it well exceeds the yield limit, consequently  $\epsilon_{11}^p$  and  $\epsilon_{22}^p$  are also large.

### 2.2.8 Modeling fatigue

A recent attempt at modelling the failure modes and include a fatigue analysis was made in 2018 at the Simon Fraser University in cooperation with Ballard Power Systems [22]. In this study, a cumulative fatigue damage model was created and evaluated, damage was approximated using Rainflow counting in combination with Palmgren-Miner's rule [19]. This is a typical industry approach and is one of the most commonly used cumulative damage equations for failures caused by fatigue. A potential disadvantage is that it assumes a simple linear life-stress relationship, which we know to not be true for PFSA PEM[23].

The main findings of the study are presented below in figure 2.11. The scope of this work was firstly to create such a model using the well studied Nafion PEM, and then to analyse how different stress magnitudes affected the lifetime. The stress magnitude stems from the swelling and water cycling [3], and so the maximum humidity was in this case varied to induce different levels of stress.

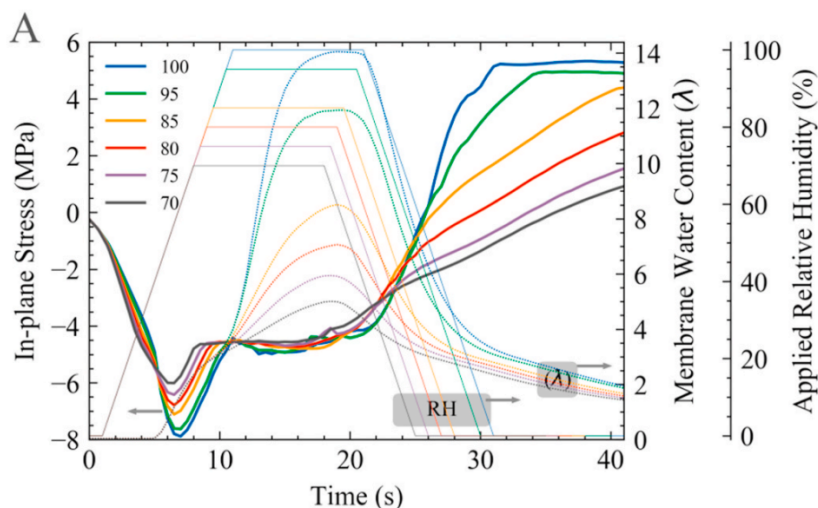


**Figure 2.11:** Stresses induced by different humidity cycles[23]

In this figure one should compare the faded lines of humidity cycling to the fuller lines of resulting stress. It was here shown that larger ranges in humidity cycles directly affected the residual tensile stress, more so than the compressive mid-cycles stress. This stress was then cycled against the failure criteria of complete rupture, with results shown in figure 2.12. In this figure the Fatigue usage factor  $F$  equal to 1 indicates total rupture and failure of the PEM. A commonly showcased result from

testing that increasing the experienced humidity  $\Delta$  (difference between largest and lowest experienced value) results in exponential loss of lifetime for the PEM [3].

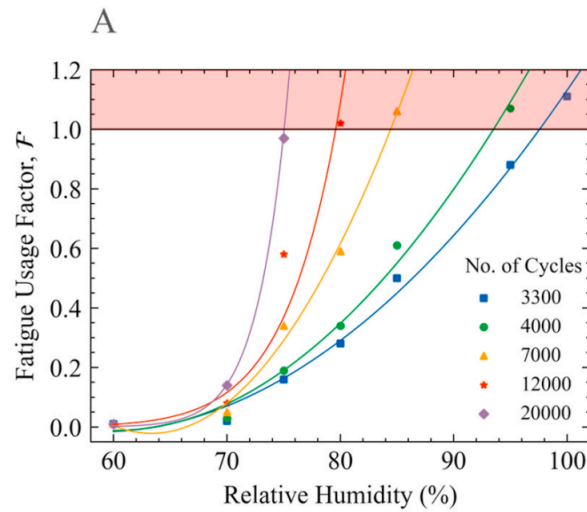


**Figure 2.12:** Fatigue factor plotted against maximum relative humidity[23]

The study shows that while modelling work of PEM is possible, it is currently limited to the most well studied membranes. Because of this, adapting it for the scope of this study to predict lifetime of novel membranes would prove difficult. The current modelling research of PEM is mostly focused on developing the understanding of how large the stresses induced become when varying parameters such temperature and humidity [2].





# 3

## Methods

The scope of this thesis is two-fold. Firstly, to add to the current understanding of PEM mechanical strength. Secondly, to create an applicable selection process for PEM with high correspondence to durability results of the DOE mechanical testing protocol.

Research done on PEM mechanical stability suggests that the dominating factor is the in-plane stress brought about by the inhibited swelling/shrinking cycle experienced by the membrane [2]. This phenomenon will be more thoroughly analysed. Research and novel material design studying this almost exclusively focus on the swelling from ambient conditions, and neglects the whole range of humidity also tested for in the DOE protocol and experienced in real operations [7]. This thesis will attempt to increase the understanding here and include such material testing and investigation.

### 3.1 Selection methodology

The selection process presented here will have two main parts, to be implemented as step one and two, with the DOE in-situ cycling to be regarded as a potential third step in an evaluation of the mechanical strength of a novel PEM.

#### 3.1.1 Part 1

The first part will present a theoretically designed model that tries to evaluate membranes based solely on ex-situ measurable material properties, such as the swelling and tensile strength. This equation will be a counterpart to the one presented by MacKinnon et al in 2009 in equation 2.3 ( $F_x$ ). While the Membrane humidity stability factor presented in 2009 was a reasonably sound framework, and a strain model is usually preferred for low-cycle fatigue, attempting a strain based fatigue analysis in an enclosed environment where the degrees of freedom are limited is ill-advised [19]. The Membrane humidity stability factor also fails to show any correlation with later in-situ testing results. The equation here presented will instead be a **stress** based model that tries to encapsulate the plastic strain component that serves to benefit a strain based model for these scenarios.

To aid the development of such a model, PowerCell Group houses a vast quantity of membranes, with many of them having known results from DOE testing. This will aid the development by having the correct ranking of the membranes available, and if a theoretically sound model also produces results that align with the later in-situ

results, it would augment the validity of the approach.

#### **3.1.2 Part 2**

The second part will be an ex-situ test developed to simulate the in-situ conditions and cycle the membrane until failure by complete fracture. The basis for investigating this test is two articles briefly mentioned earlier in section 2.2 [13],[9]. These articles both proposed variations of DMA testing, which is deemed suitable because of its ability to create a controlled environment of humidity, temperature and stress [9]. Their differing approaches have been studied and a logical continuation will here be presented for investigation.

## **3.2 Material measurements**

As mentioned earlier, PowerCell Group houses a vast quantity of PEMs, with many of them having known results from DOE testing. These membranes will have the following list of material and structural properties measured serving as a basis on which the theoretical model of part 1 will be developed.

- Tensile Strength
- Strain to fail
- Yield stress
- Yield strain
- Young's Modulus
- Energy to fail
- Swelling (80 °C, water)
- Shrinkage (60 °C,  $\approx$  5% RH)
- Thickness

These parameters are a combination of some of the most common material properties in mechanical analysis, together with those thought to be of specific interest for this topic. Most of these have been described earlier in this report, nevertheless an exhaustive list will now be presented

<i>Property</i>	<i>Definition</i>	<i>Unit</i>
Tensile Strength	The highest measured stress, the stress required to induce failure.	MPa
Strain to failure	The highest measured strain, the elongation required to induce failure.	%
Yield Stress	The stress required to initiate deformation not reversible by removal of load.	MPa
Yield Strain	The strain required to initiate deformation not reversible by removal of load.	%
Young's Modulus	The stiffness of the material for small deformations, calculated as the slope for the early regions of deformations.	MPa
Energy to failure	The energy that the specimen has absorbed up to the point of specimen failure. It is the area under the force-deflection curve from the test start to the failure point.	$\frac{J}{m^2}$
Swelling (80°C, water)	Swelling experienced from ambient conditions after submersion in a water basin.	%
Shrinkage (60°C, 5% RH)	Shrinkage experienced from ambient conditions after such analysis.	%
Thickness	Membrane thickness, usually between 8 and 20 microns, measured in ambient conditions	$\mu m$

**Table 3.1:** Material properties of interest

### 3.3 Theoretical Model

Previously referred to as Part 1, the theoretical model aims to introduce a stress based equation to supersede the Membrane humidity stability factor  $F_x$  introduced by Mackinnon in 2009. This novel model ( $F_x$ ) was correct in attempting a strain bases analysis because of the low-cycle fatigue scenario. Nevertheless, the approach was too elementary and did not capture the complexity needed to sufficiently predict later in-situ behaviour. It should also be noted that the  $F_x$  factor shows no correlation to the DOE testing results.

#### 3.3.1 Swelling stress

As previously discussed, the mechanical fatigue experienced by the PEM stems from the hygro-thermal swelling-strains of the membranes. This swelling in an enclosed spaced generates mechanical stress equivalent to the swelling prevented multiplied by the stiffness(Young's Modulus) of the PEM. We thus introduce a variable Swelling Stress calculated as:

$$\text{Swelling Stress} = \text{Total Swelling} * \text{Young's Modulus} \quad (3.1)$$

Here Total swelling is defined as swelling + shrinkage to encapsulate the total humidity span experienced by the PEM, with these properties defined as in table 3.1.

### 3.3.2 Fatigue limit

A material typically has something called a Fatigue limit, a level of stress that the component can experience for an infinite number of cycles without breaking. When doing the theoretical prediction one would want to account for variations here. A typical estimate for this fatigue limit is based on the yield limit [19], an adaptation of this will here be implemented. The original assumption by Juvinall in 2006 was to use half the yield stress as an approximation for the fatigue limit if no other reducing factors were present, with lower values being suggested for softer materials [19]. No such easily applicable model exists for plastics, both because they are generally a more complex non-linear material than metals and also not often subjects of fatigue analysis. In an attempt to capture this phenomenon without introducing a large approximation, DMA analysis was used to find the strain and stress for which the material starts to experience a loss of elasticity modulus ( $E'$ ). This value was found to be roughly half the yield stress for the subjects analysed, with a typical result showcased in figure 3.1 below.

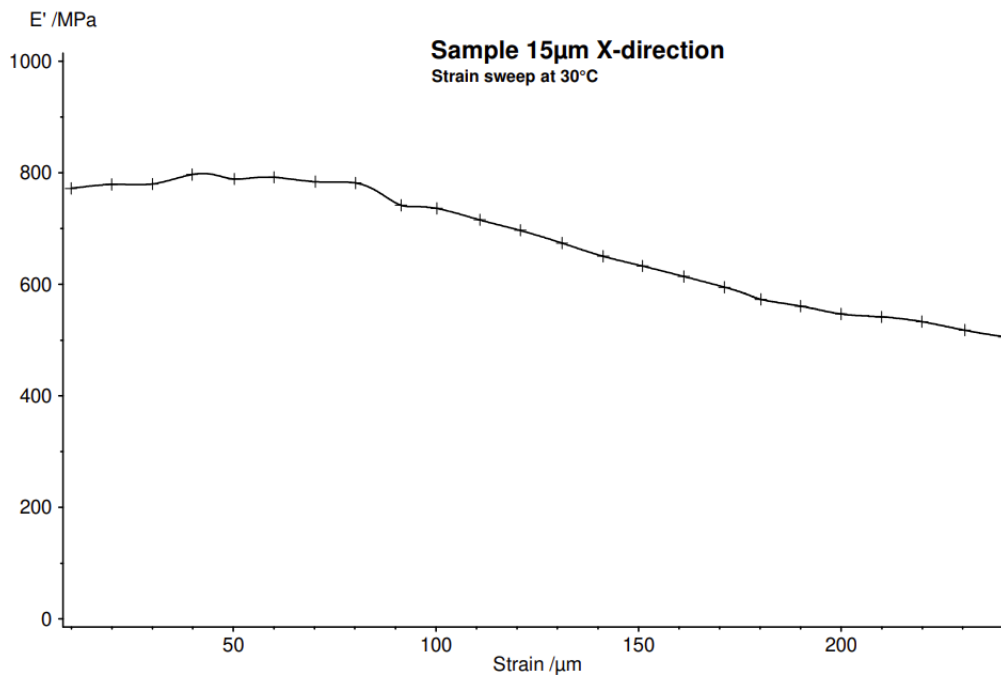


**Figure 3.1:** Strain sweep of a PEM, indicating a start of loss of elasticity at an amplitude of  $80 \mu\text{m}$  (0.8% strain)

Following these results it is suggested to conduct similar testing and use this value in the following equation, if such testing is unavailable, it is instead suggested to use half the yield stress. This value is to be subtracted from the earlier equation 3.1 to define the following *Damaging Swelling Stress*.

$$\text{Damaging Swelling Stress} = \text{Total Swelling} * \text{Young's Modulus} - \frac{\text{Yield Stress}}{2} \quad (3.2)$$

This could now be referred to as the damaging stress experienced by the membrane during each swelling cycle, incrementally adding to the accumulating fatigue damage, eventually leading to fatigue failure. The material property yield stress is not as easily defined as it would be for a more ideal material like steel. A common definition used for a more visco-elastic material like this one is the 0.2% offset-rule, visually presented in figure 3.2 below. The yield stress ( $\sigma_y$ ) used in this work will follow this 0.2% offset definition, where the stress measured at 0.2% plastic strain is taken as yield stress.

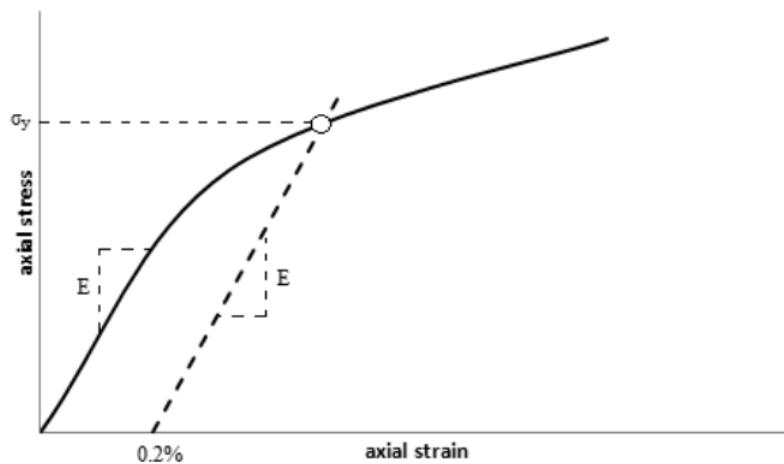


Figure 3.2: Visual definition of yield stress[19]

### 3.3.3 Mechanical failure index

Having a definition of the fatigue inflicting swelling stress, one now needs a material strength parameter to relate this stress to. Here the tensile strength has been chosen as it directly correlates to the failure mechanism chosen, fracture. We thus introduce a unitless indexing number that can be used to compare two membranes against one another, Mechanical failure index (MFI):

$$\text{MFI} = \frac{\text{Swelling stress} - \frac{\text{Yield stress}}{2}}{\text{Tensile Strength}} \quad (3.3)$$

With Swelling stress defined as in equation 3.1.

### 3.3.4 Using MFI

MFI does not directly predict the cycles until failure for any given PEM, for such a prognosis one would require a complete model of the surrounding balance-of-stack. Instead, its usage is to compare two different membranes as either better or worse than one another, just like there earlier presented humidity stability factor  $F_x$ . Thus, having a reference PEM as a minimum baseline for mechanical stability, one could readily use MFI in a first step to exclude potential novel membranes based on simple material testing. This would best be used as a first step in a down selection of candidate PEM. It is not recommended to compare top quality options using only

this as a basis for decision. For added clarity, it is noted that a *lower* MFI value is better.

## 3.4 DMA testing

The DMA test to be investigated in this study is a continuation of the testing done by T.T. Aindow in cooperation with UTC Power Corporation, presented in their article “Use of mechanical tests to predict durability of polymer fuel cell membranes under humidity cycling” [13]. In their study they proposed a solution to the problem that the stress is both generated and experienced by the PEM, creating an issue with simply cycling a set level of stress and comparing the fatigue life. In their study, their methodology was to first measure the stress generated by the PEM swelling, and then cycle it onto itself. In doing so they design an experiment which evaluates PEM durability based on the stress it inflicts on itself. For this procedure T.T. Aindow used catalyst coated membranes (CCM).

### 3.4.1 Stress measuring phase

The stress generated by the PEM during swelling has been concluded to be the main reason for the mechanical failure of PEMFC [10]. To mimic this stress ex-situ and cycle it T.T. Aindow proposed a way of measuring the stress generated by a change in humidity and temperature possible with a DMA equipped with an environment chamber. A static test by measuring the stress induced in samples held at a fixed length while changing the relative humidity. Each sample was first equilibrated at 90% RH for 100min under zero load. A nominal strain of 0.2% was then applied to straighten the sample before humidity cycling. The humidity was then stepped down to 30-10% and the DMA response was used to monitor the induced stress, this was repeated in a cyclic manner a couple of times to ensure accurate results. The purpose of this test was to establish the amplitude of the mechanical stress associated with membrane dry-out as a result of reduced humidity. This enables the fatigue response of the CCM to be correlated to its own generated stress [13]. This procedure was done at the same temperature that the later stress cycling was to be done, 60°C. Example results of this procedure are presented in figure 3.3 below.

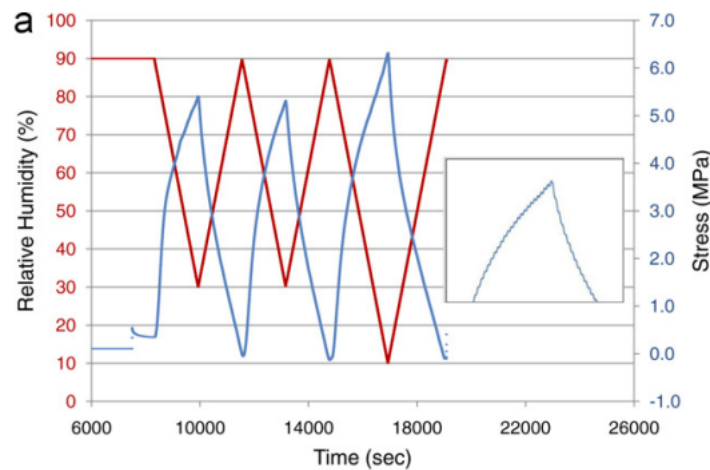


**Figure 3.3:** Stress results correlated to humidity in DMA [13]

### 3.4.2 Stress cycling phase

In the article by T.T. Aindow, mechanical fatigue testing was performed with the same DMA as the stress measuring test, again utilizing the environmental chamber. The humidity was kept at 90% and the temperature at 60°C. They propose that cycling the maximum stress measured in the earlier phase until fracture would yield a result with high correlation to the later in-situ behaviour of the PEM. They performed multiple tests, in all cases the minimum stress was set at 20% of the maximum stress, the stress was cycled using a frequency of 10 Hz [13].

#### 3.4.2.1 Results and conclusions

The results of the study performed by T.T. Aindow showcased that the PEM exhibits characteristics that are typical for polymer materials. It is discussed in the article how currently there is no validated ex-situ methodology that can be used to characterize membrane durability under humidity cycling conditions. It is further proposed that this stress test with the DMA can be translated to the amplitude of relative humidity cycling experienced in the fuel cell, and that therefore, the durability of PEM fuel cell can be estimated [13] This is a highly valuable conclusion for the field, and one that prompts further investigation.

#### 3.4.2.2 Remaining life investigation

As a continuation researched by T.T. Aindow, post-mortem analysis of cells that have not yet failed was conducted in the same way as the earlier pristine CCM. The results showcased that the degraded membranes had less than 5% cycles to fail remaining when compared to the as-delivered CCM tested earlier. Showcasing that the method could also be used to estimate the remaining lifespan, where there is also no established method in the industry.

### 3.4.3 Proposed continuation to DMA stress test

The test performed by T.T. Aindow yielded compelling results and simply using their procedure as is could already be recommended as a next step for down selection of PEM, following the earlier presented MFI. However, investigating if such testing is possible using un-coated PEM is suggested in the article as a logical continuation of the work, and so this is what will be investigated in this report. It is postulated that such testing might not be possible, as the porous catalyst layer present on the membrane readily provides a zone for crack initiation. And without this, the time until failure could vary hugely as this part of a fatigue test is prone to a high degree of randomized variations.

### 3.4.4 Procedure description

The procedure to be conducted has been discussed but for sake of clearance and ease of reproduction, it will now be summarized. The temperature has been increased from T.T. Aindow's suggested 60 to 80 C, to better mimic the in-situ temperature of modern PEMFC.

#### 3.4.4.1 Sample preparation

1. Cut samples according to the following specifications, taking extra care to ensure no jagged edges for crack initiation.

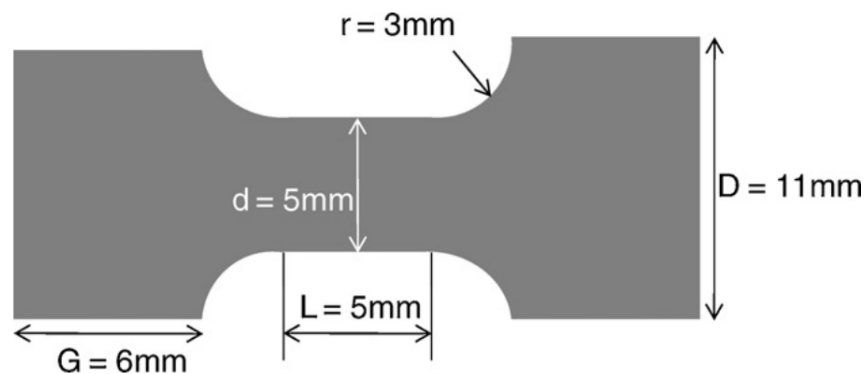


**Figure 3.4:** Schematic diagram of the dog-bone sample geometry used.

2. Condition samples in 23°C and 50%RH for minimum 40 hours.

#### 3.4.4.2 Stress measuring phase

1. Mount the sample in the DMA and condition the membrane in 80°C and 90% RH for 100 minutes without applying a load.
2. Apply a nominal force of 0.02N to straighten out the slack in the membrane.
3. Lock the position in the DMA.



4. Reduce RH to 10% and hold until a maximum resulting stress has been measured, stress is to be calculated as

$$\sigma = \frac{\text{Force}}{\text{Cross-sectional Area}} \quad (3.4)$$

#### 3.4.4.3 Stress cycling phase

1. Parameters for cyclic loading until fracture is 80°C, 90% RH (Same as stress measuring phase) and 10Hz, maximum force is to be identical as the one measured in the previous phase, minimum is set as 20% of this maximum.
2. Longitudinal and Transverse directions (the x- and y in-plane) are to be considered as separate samples.

### 3.5 Comparison with known data

Powercell Sweden houses a broad selection of PEM with known data from DOE humidity cycling test. This data will be used as a reference value for a supposed correct ranking of membranes with regards to mechanical strength. Using this correct ranking the MFI and DMA testing procedure will be evaluated based on how well the results correlate. Due to NDAs with suppliers, the names of the membranes used cannot be specified, they will instead be given an alphabetical letter for representation A -> D. In regards to ratings from DOE protocol, their values are presented in table 3.2 below. The data displayed will have normalized values to preserve sensitive information.

PEM	Normalized Rating
A	1.0
B	1.1
C	1.25
D	3.0

**Table 3.2:** DOE RH Cycling test results of reference PEM to be used for comparison with MFI and DMA results.

While the values here are normalized, they represent 1-3 times the DOE 2020 target for PEM durability under RH cycling (5000 hours).



# 4

## Results and discussion

Throughout this thesis work, a theoretical methodology has been developed and examined that combines more basic mechanical testing with more advanced fatigue and fracture analysis. Along with a continuation of an experimental approach utilizing a DMA machine. The results obtained will be presented, analyzed, and discussed in the following section. The data displayed in the graphs have been normalized to preserve sensitive information about the PEM used in this study.

### 4.1 Part 1. Theoretical model

The equation for MFI was previously shown but is here repeated for clarity:

$$\text{MFI} = \frac{\text{Swelling stress} - \frac{\text{Yield stress}}{2}}{\text{Tensile Strength}} \quad (4.1)$$

In this equation, which is an attempt to translate the information collection in the literature study into a readily usable method for PEM RH cyclic durability, the more easily measured material properties of the PEM used for an initial estimation of the later in-situ durability. The numerical results of MFI (normalized) are presented below in figure 4.1.

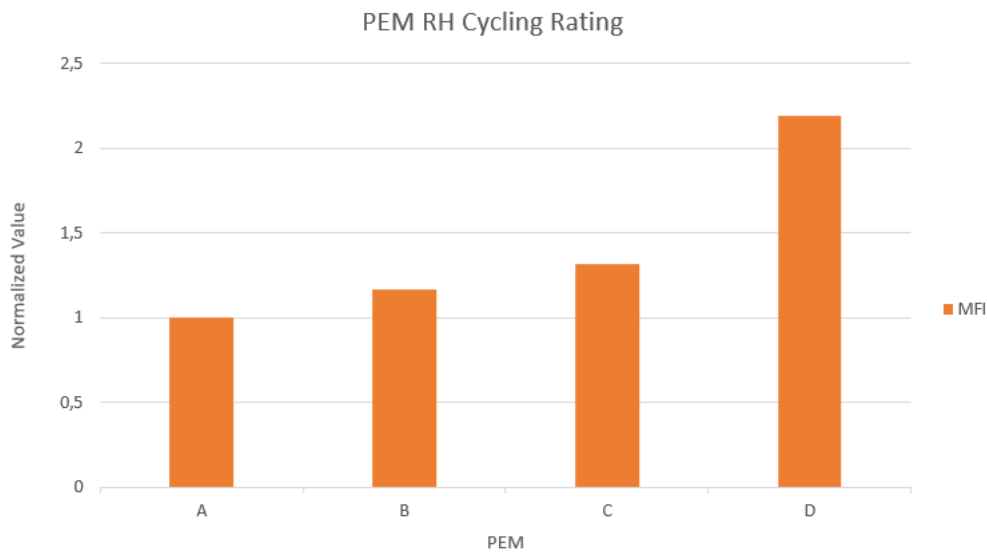


**Figure 4.1:** Normalized ( $\frac{MFI_x}{MFI_A}$ ) results for the 4 reference PEM

Note that these values are both normalized and inverted ( $\frac{1}{MFI}$ ) to be more easily understood visually, as otherwise a lower value would be better, which might be seen as less intuitive. It is here shown that the PEM follow the known ranking previously shown in table 3.2, which is exceptionally good for an ex-situ material properties model. To better illustrate how MFI compares to the later in-situ results of RH cycling, they normalized rating from the DOE testing has been added in figure 4.2.

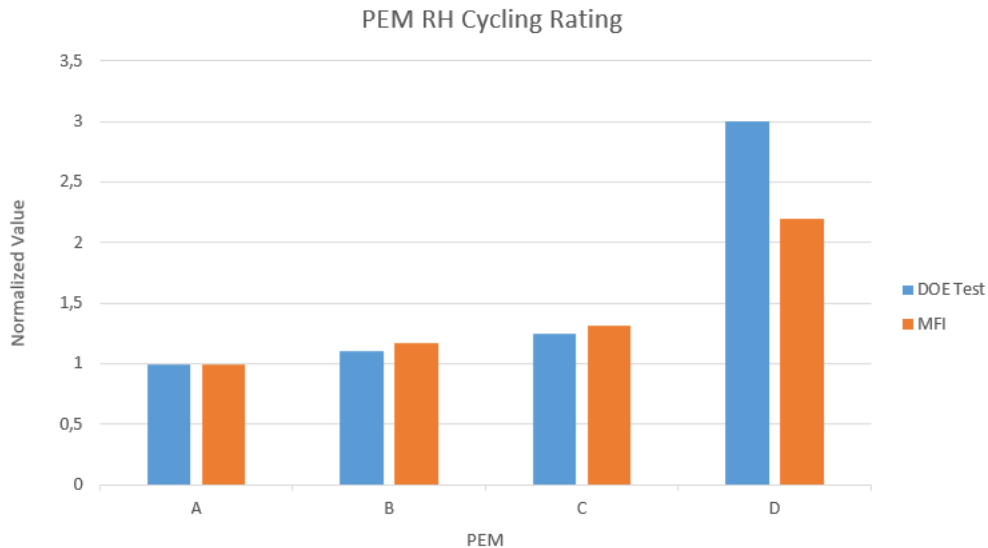


**Figure 4.2:** Results of MFI compared to DOE Testing data of the same PEM

It is here shown that the rankings predicted by MFI is in line with the DOE protocol ranking of the same PEM.

#### 4.1.1 Discussion

As noted during its introduction, MFI should not be used to gauge exact lifetime, but instead provide an initial ranking and ballpark figure and feeling about how mechanically durable one can expect a novel PEM to be in the later in-situ situation. As such what matter most is the correct “ranking” between PEM, and this is nicely showcased in figure 4.2. It is noted that the MFI numerical value for PEM D is marginally lower than what the later in-situ DOE testing showcased, but with a ranking still correct. There is a physically sound reason for this behaviour to be showcased. The equation for MFI assumes a linear relation between stress and lifetime, while this behaviour is almost always an exponential function [19]. This also explains why the MFI for B and C are higher while the prediction for D is lower, it follows a linear function while the DOE Test showcases the reality, which is exponential. This exponential relationship between stress and lifetime can easily be seen in the earlier figure 2.12. To further showcase this point, trendlines have been added to the data in figure 4.3, with MFI being linear and DOE instead showcasing the naturally exponential relation between stress and lifetime.

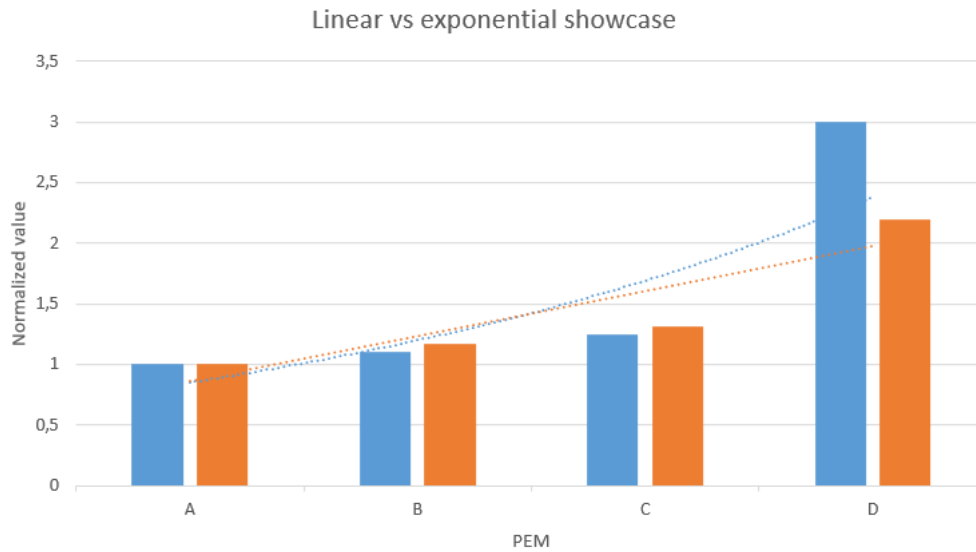


**Figure 4.3:** Illustration of the different trend lines, MFI is linear and DOE is exponential

### 4.1.2 Potential Changes

One could argue that MFI should also have an exponential form to better capture this relation between stress and lifetime, at the cost of added complexity. Seeing as the initial point of the design was to have an easy and readily available method for a first impression of mechanical strength, it was instead prioritized to have a less advanced equation for this application.

### 4.1.3 Fatigue testing

A reasonable continuation of this MFI approach would be to introduce more advanced material testing. As whenever one wants to predict fatigue and fracture behaviour, the more sophisticated equations comes at the cost of expensive material testing. An example would be conducting testing for the Fatigue limit instead of using the approximation presented here.

## 4.2 Part 2. DMA Testing

The major difference between the testing conducted here and the one done in the article referenced for inspiration, was that clean PEMs were used instead of CCMs. This meant that the ductile PEM did not have its brittle and porous coating layer. This ended up in that test did not result in the desired outcome. Unfortunately the results were varied and the reproducibility low, this data will now be presented and following the phenomena thought to be behind this variance will be discussed. Potential suggestions for continuation of work will also be reviewed.

### 4.2.1 The selection of clean PEM

To begin the choice of using un-coated PEM will again be discussed. It was suggested in the article referenced that it be done as a logical continuation of their work, and had it been successful it would be a more appropriate test for evaluating PEM. This would have been the case for two reasons, firstly, it would have introduced fewer variables which would make conclusions easier to draw. Secondly, in PEMFC industry the coating is developed after the PEM is selected, and having the same “coating” for all PEM testing would be an unfair comparison, as the coating would be a better match for some, again, complicating the process of drawing conclusions from such testing.

### 4.2.2 Stress Measurement Phase

The Pre-test of measuring the stress related to the swelling and contraction behaviour of the PEM was completed, while not all data can be presented due to an NDA, an example of results from such testing is here presented below in figure 4.4

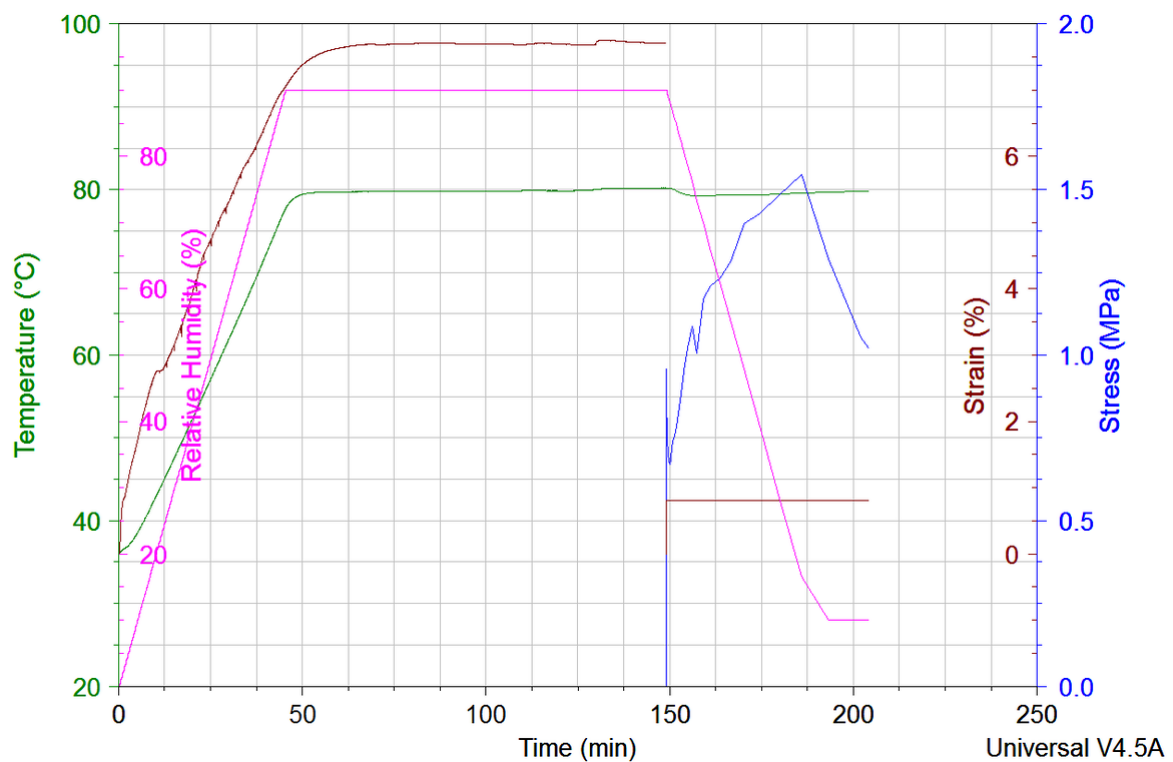


**Figure 4.4:** Stress measurement pre-test results

In this figure one can clearly see how with the ramping of temperature and humidity, the PEM elongates to >7% strain. Next the PEM is locked in place and the humidity is lowered, in turn creating a stress response from the materials shrinkage.

### 4.2.3 Stress Cycling phase

The stress cycling phase, unfortunately, did not yield reproducible data, a PEMs lifetime could vary from 1 - 40 hours between samples under similar test conditions. This resulting variance was contributed to a varying degree of defects between samples. It is generally accepted that the process of crack growth under cyclic loading is divided into three phases (see figure 4.5 below) Crack initiation, Crack propagation and Fracture [19]. Specifically, the first stage presents a threshold, below which there is no crack growth. The second stage where crack growth proceeds at a relatively steady state (usually described as Paris' Law). The final stage represents an unstable situation, where the engineering structure fails within a small number of cycles.

However, predicting crack “initiation” is far more difficult, as it is largely reliant on micro-structure defects for localized stress concentrations. This is presented as the reason for the large variance between testing results in this DMA stage, that the crack propagation was relatively swift, but that the crack initiation part for such a ductile material could vary considerably.

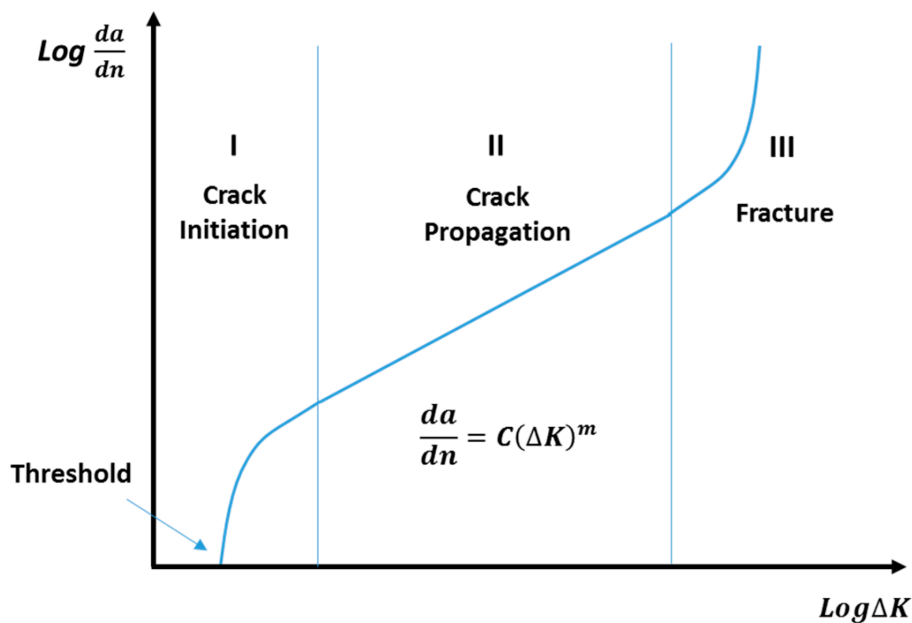


**Figure 4.5:** The 3 phases of crack growth, figure from Downing [19]

### 4.2.4 CCM and PEM comparisons

In the study presented for the source of the DMA method [13], they used CCMs, membranes coated with a brittle and porous layer, which presents a readily available zone for crack initiation. Indeed it has been shown that this coating layer shows considerable cracks after only 5% strain [24]. This compared to the 150-250 % strain at which PEMs start to show crack initiation. This key difference in using a CCM would provide a an almost immediate crack in the stress cycling, making the linear and more reproducible crack growth phase become the majority of the test. The

results in their report show a high degree of repeatability, here showcased in figure 4.6 below, consistent with this reasoning.

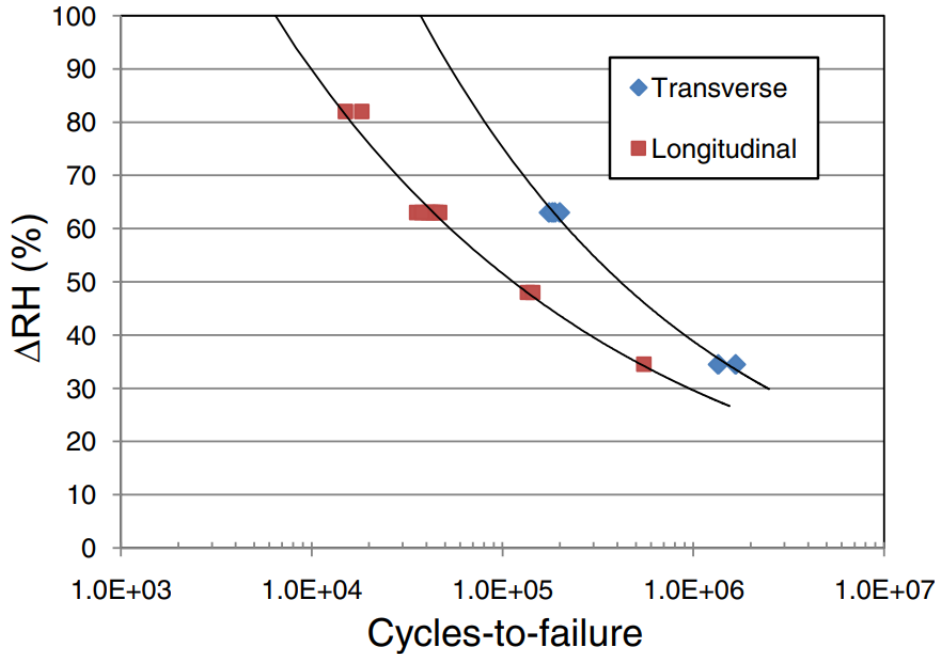


Figure 4.6: Results from article[13]

### 4.3 Conclusions

A theoretical methodology for the characterization of mechanical durability in PEMFC membranes under humidity cycling has been presented. It has been shown that the stress state and resilience that the membrane experiences during the humidity cycling, which arises as a result of load cycling in a fuel cell environment, can be predicted using basic material testing parameters. Thus, such testing can be used to evaluate membrane failure resistance under relative humidity cycling. In addition, a continuation of an already tested method for fatigue testing was tried and evaluated. While this was deemed unsuccessful as the reproducibility was too low. The low reproducibility was contributed to the high variance in sample micro-structure, resulting in unpredictable crack initiation. Investigating this also yielded valuable insight into PEM mechanical durability.



# Bibliography

- [1] Jules Verne. *The mysterious island*. ISBN: 9781840226249.
- [2] Ahmet Kusoglu and Adam Z. Weber. “New Insights into Perfluorinated Sulfonic-Acid Ionomers”. In: *Chemical Reviews* 117.3 (Feb. 2017), pp. 987–1104. ISSN: 15206890. DOI: 10.1021/acs.chemrev.6b00159.
- [3] Adam Z Weber. *Proton-Exchange Membrane Fuel Cells Fuel Cell Engineering*. Tech. rep. 2017.
- [4] Lu Zhang et al. “Modeling and Experimental Investigation of the Anode Inlet Relative Humidity Effect on a PEM Fuel Cell”. In: *Energies* 15.13 (July 2022). ISSN: 19961073. DOI: 10.3390/en15134532.
- [5] Ibrahim Hadi Tawil and Matook A M. *FUEL CELLS-THE ENERGY KEY OF FUTURE-Review and Prospective Study control of Electric Machine View project Development, Modeling and Evaluation of Solar Energy Operated AB/AD-sorption Cooling Systems View project FUEL CELLS-THE ENERGY KEY OF FUTURE Review and Prospective Study Academy of Graduate Studies*. Tech. rep. 2008. URL: <https://www.researchgate.net/publication/323401704>.
- [6] Alexander Trattner, Manfred Klell, and Fabian Radner. “Sustainable hydrogen society – Vision, findings and development of a hydrogen economy using the example of Austria”. In: *International Journal of Hydrogen Energy* 47.4 (Jan. 2022), pp. 2059–2079. ISSN: 0360-3199. DOI: 10.1016/J.IJHYDENE.2021.10.166.
- [7] A. G. Olabi, Tabbi Wilberforce, and Mohammad Ali Abdelkareem. “Fuel cell application in the automotive industry and future perspective”. In: *Energy* 214 (Jan. 2021). ISSN: 03605442. DOI: 10.1016/J.ENERGY.2020.118955. URL: [https://www.researchgate.net/publication/344540084\\_Fuel\\_cell\\_application\\_in\\_the\\_automotive\\_industry](https://www.researchgate.net/publication/344540084_Fuel_cell_application_in_the_automotive_industry).
- [8] “GM marks 50 years of FCEV development, from Electrovan to Chevrolet Colorado ZH2”. In: *Fuel Cells Bulletin* 2016.11 (Nov. 2016), pp. 14–15. ISSN: 1464-2859. DOI: 10.1016/S1464-2859(16)30330-3.
- [9] Ramin M.H. Khorasany et al. “Mechanical degradation of fuel cell membranes under fatigue fracture tests”. In: *Journal of Power Sources* 274 (Jan. 2015), pp. 1208–1216. ISSN: 03787753. DOI: 10.1016/j.jpowsour.2014.10.135.
- [10] DOE. *3.4 Fuel Cells*. Tech. rep. 2017. URL: [http://energy.gov/sites/prod/files/2015/10/f27/fcto\\_2014\\_market\\_report.pdf](http://energy.gov/sites/prod/files/2015/10/f27/fcto_2014_market_report.pdf)., <https://www.daimler.com/documents/company/other/daimler-corporateprofile-en-2015.pdf>..

- [11] Yijing Xing, Haibin Li, and George Avgouropoulos. “Research progress of proton exchange membrane failure and mitigation strategies”. In: *Materials* 14.10 (May 2021). ISSN: 19961944. DOI: 10.3390/ma14102591.
- [12] Paul C. Okonkwo et al. “Nafion degradation mechanisms in proton exchange membrane fuel cell (PEMFC) system: A review”. In: *International Journal of Hydrogen Energy* 46.55 (Aug. 2021), pp. 27956–27973. ISSN: 0360-3199. DOI: 10.1016/J.IJHYDENE.2021.06.032.
- [13] T. T. Aindow and J. O’Neill. “Use of mechanical tests to predict durability of polymer fuel cell membranes under humidity cycling”. In: *Journal of Power Sources* 196.8 (Apr. 2011), pp. 3851–3854. ISSN: 03787753. DOI: 10.1016/j.jpowsour.2010.12.031.
- [14] Anna H. Carlsson and Ludwig Joerissen. “Accelerated Degradation of Perfluorinated Sulfonic Acid Membranes”. In: *ECS Transactions* 25.1 (Sept. 2009), pp. 725–732. ISSN: 1938-5862. DOI: 10.1149/1.3210624.
- [15] Carolin Klose. *Dissertation zur Erlangung des Doktorgrades der Technischen Fakultät der Albert-Ludwigs-Universität Freiburg im Breisgau Novel polymer electrolyte membrane compositions for electrolysis and fuel cell systems*. Tech. rep.
- [16] Ho Young Jung and Jung Won Kim. “Role of the glass transition temperature of Nafion 117 membrane in the preparation of the membrane electrode assembly in a direct methanol fuel cell (DMFC)”. In: *International Journal of Hydrogen Energy* 37.17 (Sept. 2012), pp. 12580–12585. ISSN: 03603199. DOI: 10.1016/j.ijhydene.2012.05.121.
- [17] Roderic Lakes. “Viscoelastic materials”. In: *Viscoelastic Materials* 9780521885683 (Jan. 2009), pp. 1–461. DOI: 10.1017/CB09780521885683.
- [18] “Introduction to Tensile Testing”. In: (2004). URL: [www.asminternational.org](http://www.asminternational.org).
- [19] Norman E. Dowling. *Mechanical Behavior of Materials*.
- [20] Astm International and files indexed by mero files. *Standard Test Method for Tensile Properties of Thin Plastic Sheeting 1*. Tech. rep.
- [21] S. M. MacKinnon et al. “Fuel Cells - Proton-Exchange Membrane Fuel Cells | Membranes: Design and Characterization”. In: *Encyclopedia of Electrochemical Power Sources*. Elsevier, Jan. 2009, pp. 741–754. ISBN: 9780444527455. DOI: 10.1016/B978-044452745-5.00905-9.
- [22] Narinder Singh Khattri et al. “Residual fatigue life modeling of fuel cell membranes”. In: *Journal of Power Sources* 477 (Nov. 2020). ISSN: 03787753. DOI: 10.1016/j.jpowsour.2020.228714.
- [23] Meredith N. Silberstein and Mary C. Boyce. “Hygro-thermal mechanical behavior of Nafion during constrained swelling”. In: *Journal of Power Sources* 196.7 (Apr. 2011), pp. 3452–3460. ISSN: 03787753. DOI: 10.1016/j.jpowsour.2010.11.116.
- [24] Yusuke Kai et al. “Crack formation in membrane electrode assembly under static and cyclic loadings”. In: *Journal of Fuel Cell Science and Technology* 10.2 (2013). ISSN: 1550624X. DOI: 10.1115/1.4023878.